Published in final edited form as:

Angew Chem Int Ed Engl. 2021 January 25; 60(4): 1714–1726. doi:10.1002/anie.202007668.

Stereoinduction in Metallaphotoredox Catalysis

Alexander Lipp[#], **Shorouk O. Badir**[#], **Gary A. Molander**

Department of Chemistry, Roy and Diana Vagelos Laboratories University of Pennsylvania, 231 S. 34th Street, Philadelphia, PA 19104-6323 (USA)

[#] These authors contributed equally to this work.

Abstract

Metallaphotoredox catalysis has evolved into an enabling platform to construct C(sp^3)-hybridized centers under remarkably mild reaction conditions. The cultivation of abundant radical precursor feedstocks has significantly increased the scope of transition-metal-catalyzed cross-couplings, especially with respect to C(sp^2)–C(sp^3) linkages. In recent years, considerable effort has been devoted to understanding the origin of stereoinduction in dual catalytic processes. In this context, Ni- and Cu-catalyzed transformations have played a predominant role exploiting this mode of catalysis. Herein, we provide a critical overview on recent progress in enantioselective bond formations enabled by Ni- and Cu-catalyzed manifolds. Furthermore, selected stereochemical control elements within the realm of diastereoselective transformations are discussed.

Graphical Abstract

gmolandr@sas.upenn.edu.

Conflict of interest

The authors declare no conflict of interest.

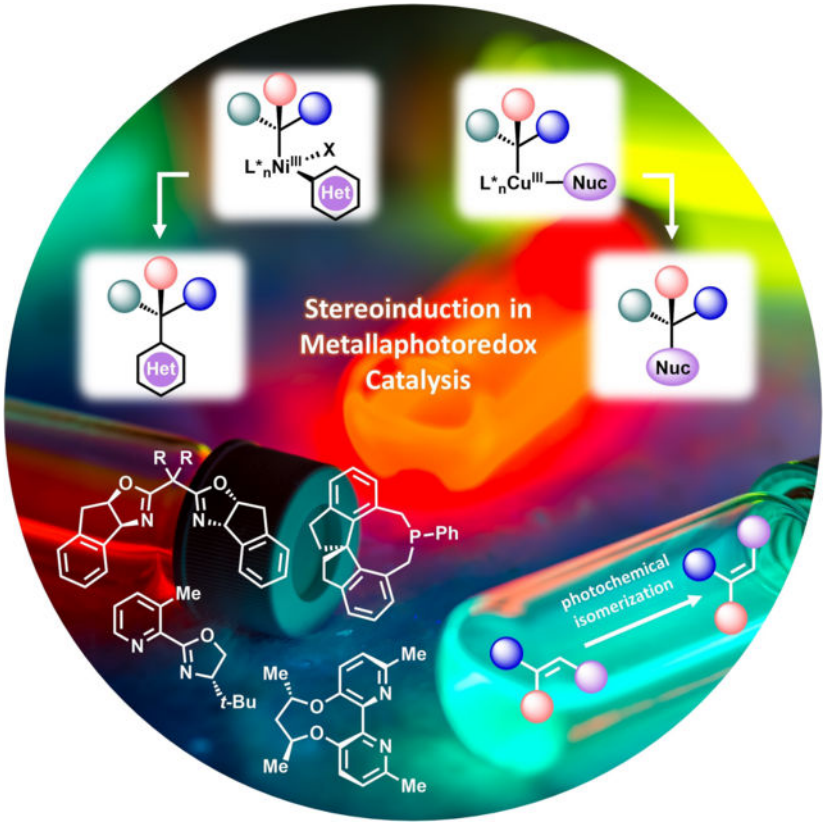

Keywords

cross-coupling; energy transfer; photocatalysis; radical precursors; stereoinduction

1. Introduction

Metallaphotoredox catalysis has emerged as a valuable advance for the rapid assembly of challenging C–C linkages under mild reaction conditions.[1] Upon excitation with visible light, a photocatalyst engages in single-electron transfer (SET) events, generating reactive radical intermediates that get funneled into a transition-metal cycle for further functionalization (Figure 1). Owing to the strong correlation between the proportion of C(sp^3)-hybridized centers in drug candidates and their ultimate probability of clinical success,[2] metallaphotoredox catalysis has gained traction in medicinal chemistry discovery efforts.

In recent years, the use of chiral ligand scaffolds has enabled new avenues for asymmetric bond disconnections in photochemical systems.[3] Although progress has been made, stereoselective reactions remain synthetically underexplored. Furthermore, mechanistic gaps persist with respect to the origin of stereoinduction. In this Minireview, we examine recent progress in photoinduced Ni- and Cu-catalyzed enantioselective transformations. Although there are numerous substrate-controlled, diastereoselective processes in metallaphotoredox catalysis, we highlight examples in which ligand effects and photochemical isomerization

events are used to direct the stereochemical outcome. To provide a complete overview, we also address the current limitations and speculate upon future opportunities that might be amenable under similar mechanistic paradigms.

2. Enantioselective Transformations

2.1. Ni-Catalyzed Enantioselective Transformations

In 2014, our group demonstrated the first photoredox/Ni dual catalytic system to construct $C(sp^2)$–$C(sp^3)$ linkages under remarkably mild reaction conditions with high functional group tolerance (Scheme 1A).[1a] In this seminal report, we established that benzyltrifluoroborates ($E_{1/2}$ =+1.10 V vs. SCE) undergo oxidative fragmentation to deliver alkyl radicals that function as suitable partners in Ni-catalyzed cross-couplings. Simultaneously, the MacMillan and Doyle groups disclosed similar catalytic strategies through photoredox/Ni decarboxylative and $C(sp^3)$-H arylation platforms.[1b] In stark contrast to traditional two-electron transmetalation processes,[4] single-electron transfer (SET) enables the introduction of $C(sp^3)$-hybridized carbons under inherently low activation energy barriers, circumventing the need for strong bases or reactive, pyrophoric reagents.[1e–i]

To probe the mechanistic intricacies of this unprecedented paradigm, density functional theory (DFT) calculations were conducted to deduce the order of radical addition to the Ni center with respect to oxidative addition.[5] Although both mechanistic scenarios outlined in Scheme 1B give rise to an identical high-valent Ni^{III} intermediate (**F**), the formation of alkylNi(I) species **E** through an initial radical capture event proceeds via a lower energy barrier. Subsequent reductive elimination and single-electron transfer from the reduced state of the photocatalyst to a Ni^{I} complex regenerates both catalytic cycles. Most notably, these calculations suggest that the stereodetermining step in this manifold is reductive elimination. As such, radical combination is governed by Curtin–Hammett conditions whereby one of two equilibrating diastereomeric Ni^{III} intermediates proceeds to yield the desired C–C bond more rapidly. Utilizing a chiral bis(oxazoline) (BOX) ligand, modest enantioselectivity was observed (50% *ee*) when subjecting a racemic α-methylbenzyltrifluoroborate mixture to the reaction conditions.[1a] This observed stereoconvergence validated for the first time the merger of photoredox catalysis with asymmetric transition-metal-catalyzed cross-couplings. In subsequent studies, we demonstrated that α-trifluoromethyltrifluoroborates engage in cross-coupling with a variety of aryl and heteroaryl bromides, again with modest enantioselectivity levels (up to 60% *ee*) in the presence of a chiral BOX ligand (Scheme 2A).[6] We further showcased that enantioenriched α-alkoxy ketones can be accessed in excellent chemical yields (91%) and moderate enantioselectivities (62% *ee*) using 2,2′-isopropylidenebis[(4*R*)-4-benzyl-2-oxazoline] as a chiral ligand scaffold (Scheme 2B).[7]

Since our initial report, the Doyle and Rovis groups exemplified an elegant asymmetric Ni-catalyzed desymmetrization of *meso*-succinic anhydrides using benzyltrifluoroborates as the alkyl radical feedstock (Scheme 3A).[8] With this set of substrates, UV/Vis studies provided evidence for an enantiodetermining oxidative addition process occurring prior to radical addition to a Ni^{II} intermediate, undoubtedly a result of the more facile oxidative addition to anhydrides when compared to aryl bromides of previous studies. Although a variety of

electronically distinct primary benzyltrifluoroborates were efficiently incorporated, stereoinduction with respect to secondary benzylic systems or other secondary unactivated derivatives was not examined. Notably, inferior stereochemical control was observed when $Ni(COD)_2$ was replaced with bench-stable Ni^{II} precatalysts. Shortly after, Xiao and co-workers reported a desymmetrizing C-O coupling (Scheme 3B). A chiral 2,2′-bipyridine ligand was harnessed to offer enantioenriched 1,4-benzodioxanes.[9] The scope of the electrophile was limited to aryl iodides, presumably facilitating oxidative addition.

In 2016, the MacMillan and Fu groups investigated the feasibility of an enantioselective decarboxylative arylation procedure with another class of radical precursors, namely *N*-CBz- and *N*-Boc-protected α-amino acids (Scheme 4A).[10] A wide array of enantioenriched benzylic amines (with up to 93% *ee*), including pharmaceutically relevant derivatives, were synthesized efficiently, exploiting a chiral cyano-BOX ligand. Although this advancement presented a milestone in its own right, this approach is mainly restricted to heteroatom-stabilized radicals as well as aryl bromide electrophiles bearing electron-withdrawing substituents. A single example of an electron-neutral aryl iodide offered the desired product in modest *ee* (66%) and acceptable chemical yield (64%). Under a similar paradigm, Davidson and co-workers developed an enantioselective synthesis of *N*-benzylic heterocycles from stabilized carboxylic acids using an organic photocatalyst and a chiral pyridine-oxazoline (PyOx) ligand (Scheme 4B).[11] Limitations in the electronic profile of the electrophile persist, with trace product observed in the case of electron-rich aryl bromides. A directing group tethered to the C2 position of the heterocyclic moiety resulted in enhanced stereoselectivity, presumably because of coordination with the Ni center.

Recently, the direct functionalization of $C(sp^3)$–H bonds has enabled the rapid diversification of abundant chemical feedstocks, bypassing the need for redundant synthetic manipulations.[12] In 2017, the Doyle group utilized a chiral BOX ligand to achieve promising enantioinduction (one example displayed, 30% *ee*) in the coupling of stabilized prochiral radicals with 4-iodotoluene, stemming from a direct C–H activation of *N*-phenylpyrrole.[13] Shortly after, the Martin group exploited the use of diaryl ketones as triplet state photosensitizers for hydrogen-atom transfer (HAT) and single-electron reduction processes (Scheme 5).[14] Under the optimized reaction conditions, a wide array of cyclic and acyclic ether derivatives served as amenable partners for cross-coupling with diverse aryl and heteroaryl bromides. To exploit the power of this catalytic approach further, the authors identified a chiral cyano-BOX ligand core to induce an asymmetric coupling in moderate yields and enantioselectivities (one example displayed, 54% *ee*). Although, based on mechanistic studies using a different ligand system, the authors proposed a mechanistic pathway in which oxidative addition occurs first for the racemic transformation, initial radical combination with a Ni^0 species can perhaps not be totally ruled out.[5] In a subsequent report, the group further extended their efforts to studying an enantioselective $C(sp^3)$-H arylation of benzamides with organic halides, maintaining excellent chemo- and stereoselectivity.[15] Notably, the alkyl feedstock in both protocols is limited to heteroatom-stabilized radicals.

Another example of asymmetric synthesis via $C(sp^3)$-H functionalization was disclosed by Lu and co-workers, who demonstrated an enantioselective $C(sp^3)$-H arylation of benzylic

bonds toward 1,1-diaryl alkanes using chiral bis(imidazoline) ligands (Scheme 6).[16] A diverse set of alkylbenzene derivatives was coupled with aryl bromides under redox-neutral and mild reaction conditions. Mechanistically, the authors proposed an initial oxidative addition of the aryl halide with the metal center to generate an arylNi^{II} bromide species. Photoinduced single-electron oxidation of this intermediate delivers a bromine radical and concurrently reduces the excited state of the photocatalyst. Upon HAT, benzylic radicals are intercepted by Ni^{II} followed by reductive elimination to furnish the chiral products. Notably, a plausible energy transfer (ET) process to generate a bromine radical is well-precedented and cannot be excluded without further compelling mechanistic evidence.[17] In this scenario, the benzylic radical generated would engage the Ni^{0} complex to afford a benzylic Ni^{I} species. Subsequent oxidative addition to the aryl halide generates Ni^{III} complex **G**, with reductive elimination again leading to the coupled product. The versatility of this method was emphasized through the elaboration of complex targets.

More recently, the Mao and Walsh groups developed an asymmetric cross-coupling of α-chloro esters with aryl iodides (Scheme 7A).[18] A commercially available organic photoreductant, Hantzsch ester (HEH), was employed in lieu of stoichiometric metals such as Zn and Mn. Diverse α-aryl esters were obtained in good yields and excellent enantioselectivities (up to 94%), harnessing a chiral BOX ligand. Notably, the reaction proceeds using the organic dye 1,2,3,5-tetrakis(carbazol-9-yl)-4,6-dicyanobenzene (4CzIPN) as a photocatalyst. Other reactivity modes for delivering defined stereochemical outcomes under organic photoredox catalysis rely on embedding a triplet state photosensitizer within chiral ligand scaffolds. A recent example was published by Xiao, whereby a thioxanthone motif was linked to a chiral BOX ligand to induce an enantioselective aerobic oxidation of β-ketoesters and β-ketoamides toward diverse α-hydroxy-β-dicarbonyl products with high efficiency (Scheme 7B).[19]

Direct excitation of redox-active radical precursors, without the necessity for an exogenous photocatalyst, offers new avenues in Ni-catalyzed asymmetric transformations. Melchiorre et al. validated the use of 1,4-dihydropyridines (1,4-DHPs) as potent photoreductants to achieve this goal (Scheme 8).[20] Upon excitation at 405 nm, the corresponding alkylin DHP ($E_{1/2}$ = −1.6 V vs. Ag/Ag^{+} in MeCN) participates in two sequential SET events with a Ni^{II} precatalyst to generate the desired active Ni^{0} species and a radical cation. The latter undergoes a homolytic fragmentation to deliver a secondary alkyl radical. At this point, oxidative addition of the symmetric anhydride to the Ni^{0} center occurs followed by radical trapping to yield an acylNi^{III} complex. Reductive elimination furnishes the desired chiral ketone products. Stereochemical control is achieved via the implementation of a chiral BOX ligand. To complete both catalytic cycles, another SET event takes place from the excited state of the organic reductant to a Ni^{I} complex.

In addition to Ni-catalyzed monofunctionalizations, the Wang group reported an asymmetric acyl-carbamoylation of alkenes (Scheme 9).[21] The authors hypothesized that photoexcitation of tetrabutylammonium decatungstate (TBADT) at 390 nm generates *[W]$^{4-\bullet}$, a reactive HAT reagent key to the formation of the desired acyl radicals from aldehydes. Upon radical combination with a low-valent Ni^{0} species, oxidative addition of the carbamoyl chloride forms acylNi^{III} intermediate **F**. The authors propose that a

stereodetermining migratory insertion step with the appended olefin precedes reductive elimination to yield functionalized enantioenriched oxindoles. However, rapid oxidative addition of the electrophile followed by radical trapping is also plausible and cannot be eliminated without rigorous mechanistic/computational studies. A phosphinooxazoline (PHOX) ligand is crucial to accomplishing a high degree of stereoselectivity.

2.2. Cu-Catalyzed Enantioselective Transformations

2.2.1. Photoinduced Transformations

Owing to their ability to absorb light in the visible spectrum, to engage in SET processes, and to function as Lewis acids, Cu complexes with chiral ligands have been recognized as promising catalysts for stereoselective photoinduced transformations.[22] They are formed in situ from an inexpensive Cu source and a chiral ligand that governs the stereochemical outcome. The predominant mechanistic paradigm relies on radical generation through oxidative quenching of a photoexcited Cu^{I} complex (Scheme 10).[22a] Product formation presumably proceeds via radical addition to Cu^{II} and reductive elimination from an intermediate Cu^{III} species (**D**).

In 2016, Fu and Peters pioneered this field by disclosing an enantioselective C-N cross-coupling of racemic tertiary α-chloroamides with carbazoles and indoles (Scheme 11).[23] Even though such enantioconvergent transformations with tertiary alkyl halides as electrophiles are challenging,[23,24] excellent enantiomeric ratios were obtained using this radical approach (typically >90% *ee*). The protocol is limited to the aforementioned amines as nucleophiles (only C3-substituted indoles were employed), but offers a broad scope with respect to the electrophile, which can accommodate both aliphatic and aromatic α-substituents.

Interposing a Giese-type addition prior to formation of the Cu^{III} intermediate offers a promising approach to stereoselective alkene difunctionalizations. Along these lines, Wang and Xu disclosed a protocol for the enantioselective cyanation/fluoroalkylation of styrenes (Scheme 12A).[25] Radical generation from fluoroalkyl iodides through oxidative quenching of a photoexcited Cu^{I} complex significantly expanded the scope of a previous (thermal) protocol[26] that was limited to trifluoromethyl radicals obtained from TogniQs reagent. Following the same mechanistic principle, asymmetric alkylation/alkynylation and arylation/alkynylation of styrenes were accomplished using appropriately ligated Cu^{I}-acetylides (Scheme 12B).[27] Even though this method is limited to styrene derivatives without additional substituents on the alkene, it offers access to structurally diverse products by tolerating a range of alkyl-, aryl-, heteroaryl-, and silylacetylenes as well as various (primary) aliphatic and aromatic iodides.

An alternative mechanistic concept can be envisioned in which oxidative generation of radicals and product formation occur in two distinct catalytic cycles. Thus, in 2018, Gong reported the Cu^{II}-catalyzed enantioselective alkylation of *N*-sulfonylimines and selected ketimines using benzyltrifluoroborates as radical precursors (Scheme 13).[28] Because direct SET between the latter and Cu^{II} is thermodynamically unfavorable, radical formation through ligand exchange and subsequent light-induced homolysis was suggested.[22a,28]

Reaction of the so-formed alkyl radical with the prochiral Cu-bound imine (**E**) occurs from the sterically less shielded side, which accounts for the high enantiomeric purities of the obtained amines. A mechanistic paradigm operating through a single catalytic cycle comprising light-induced homolysis in an excited pentacoordinated ligand/Cu^{II}/imine/alkyl complex cannot be excluded.[28] The carbonyl group in the α-position of the imine is a prerequisite, reflecting the importance for strong coordination to the transition metal. Although excellent enantiomeric ratios (>90% *ee*) were obtained for primary benzyltrifluoroborates with electron-withdrawing substituents, electron-rich substitution patterns resulted in slightly diminished optical purities. The reaction proceeded smoothly with secondary benzyl- and tertiary alkyltrifluoroborates, albeit with limited stereocontrol (24–59% *ee*), indicating a decreased capability of the catalyst/ligand to discriminate between the individual substituents in these cases.

The same type of stereoinduction was exploited in an enantioselective α-aminoalkylation of benzylic *N*-acylhydrazones, furnishing products that could be transformed into 1,2-diamines by subsequent treatment with Raney nickel (Scheme 14).[29] Radical generation from secondary or tertiary α-silylarylamines through direct SET with Cu^{II} and subsequent desilylation furnish a stabilized α-amino radical that attacks the Cu-bound hydrazone (**D**). A slightly elevated temperature (25 °C instead of −40°C) was required to promote the reaction of an aliphatic hydrazone (only one investigated), which might account for the low degree of stereoinduction (19% *ee*) for this substrate. Addition of an Ir^{III} photocatalyst accelerated the reaction and enabled the use of non-silylated dimethylarylamines, presumably because of a broader redox potential window.[29]

2.2.2. Photoredox/Cu Dual Catalysis

Merging photoredox and Cu catalysis offers new avenues for stereoselective transformations by providing a dual catalytic manifold in which efficient radical generation and stereocontrolled product formation generally occur in two separate cycles.[3d,30]

In 2015, Li reported the enantioselective alkynylation of *N*-aryl-1,2,3,4-tetrahydroisoquinolines under visible-light irradiation (Scheme 15).[31] Reductive quenching of a photoexcited Ir^{III} catalyst furnishes an amine radical cation, which is subsequently converted to an iminium ion that is intercepted by a Cu^{I}-acetylide complex. The latter could be formed in situ from alkyl-, aryl-, and silylacetylenes, thereby allowing structural diversity despite the significant limitation with respect to the amine motif. The observed product formation in the absence of either light or Ir^{III} can presumably be explained by CuQs own SET chemistry. The arylation of *N*-aryl-1,2,3,4-tetrahydroisoquinolines with arylboronic acids was accomplished using a similar protocol, albeit with moderate enantioselectivity (26–80% *ee*).[32]

Stereoselective cyanation is arguably the most frequently exploited transformation in asymmetric Cu/photoredox dual catalysis (Scheme 16). Oxidative quenching of the excited photocatalyst furnishes an alkyl radical that adds to a ligand/$Cu^{II}(CN)_2$ complex (**E**). Reductive elimination from a high-valent Cu^{III} species (**F**) yields the desired alkyl nitrile, whereby the stereochemical outcome is governed by the chiral ligand.[33]

Lin and Liu disclosed a Cu^{I}-catalyzed decarboxylative cyanation of secondary benzylic *N*-hydroxyphthalimide (NHP) esters with TMSCN (Scheme 17A).[34] Although the employed asymmetric Cu^{I} complex failed to accomplish radical generation under visible-light irradiation, a dual catalytic approach encompassing an additional Ir^{III} catalyst promoted the desired transformation with high yields. Circulating the reaction mixture between a batch reservoir and a flow manifold allowed a significant scale-up of the transformation (35 g of product obtained). Furthermore, this robust protocol tolerates various functional groups, including $C(sp^2)$-halides, (thio)ethers, esters, ketones, alkenes, alkynes, arylboronic acid pinacol esters (Ar-BPin), as well as electron-rich and electron-deficient heterocyclic scaffolds. However, low enantioselectivities were reported for NHP esters derived from secondary aliphatic carboxylic acids (no exact values were given for yield and *ee*).

Enantioselective access to elaborated benzyl nitriles could be accomplished by trapping the initially formed alkyl radicals through Giese-type addition to styrenes prior to formation of the Cu^{III} intermediate (Scheme 17B).[35] Primary, secondary, and tertiary aliphatic NHP esters proved to be suitable radical precursors for this dual catalytic three-component reaction. Aliphatic alkenes afforded only trace amounts of the desired product, and neither α- nor β-substituents on the styrene were reported. Employing redox-active propargyl esters as radical precursors further expanded this general reaction paradigm to the synthesis of secondary propargyl nitriles with excellent functional group tolerance (Scheme 17C).[33] In this case, DFT calculations suggest that formation of the high-valent Cu^{III} species through radical addition to the transition metal is reversible and that stereoselectivity results from different energy barriers for reductive elimination.

Following the same mechanistic principle, radical generation through reductive ring-opening of 2-arylcyclopentanone oxime esters enabled stereoselective synthesis of 1,4-dicarbonitriles (Scheme 18A).[36] Low yields were obtained in the absence of either light or photocatalyst, indicating that even though CuQs own SET chemistry is able to promote this transformation, efficiency can be significantly increased by using a dual catalytic approach. Elevated temperatures (50 °C) afforded reasonable yields without the need for an additional photocatalytic cycle, albeit with slightly diminished enantioselectivity. Both electron-donating and electron-withdrawing substituents on the arene were well tolerated (typically >90% *ee*), and the products could be converted into the corresponding 1,6-diamines by treatment with borane–THF without loss in optical purity. The analogous synthesis of asymmetric 1,3-dicarbonitriles proceeded smoothly even at low temperatures (10 °C) and without a photoredox catalyst, presumably because of the increased ring strain in 2-arylcyclobutanone oxime esters.[36] A similar ring-opening cyanation was disclosed by Chen and Xiao.[37]

Reduction of *N*-alkoxypyridinium salts and subsequent intramolecular 1,5-hydrogen atom transfer (1,5-HAT) furnish alkyl radicals that can engage in cascade processes such as azidation, thiocyanation, and cyanation to yield δ-functionalized alcohols.[38] The potential of the developed protocol for asymmetric transformations was demonstrated by the enantioselective synthesis of a δ-hydroxynitrile (Scheme 18B). Along the same lines, enantioselective access to δ-hydroxynitriles was accomplished starting from the corresponding primary *N*-alkoxyphthalimides.[39] This method is limited to the synthesis of

2-aryl-5-hydroxynitriles, presumably reflecting the need for an appropriately positioned benzylic C–H bond to accomplish efficient intramolecular 1,5-HAT.

Exploiting the advantages of a dual catalytic approach, Gong and co-workers expanded the pool of suitable radical precursors for their previously[28] developed alkylation of *N*-sulfonylimines (Schemes 13 and 19).[40] Using commercially available 5,7,12,14-pentacenetetrone (PT) as an organic photocatalyst enabled the generation of benzylic, allylic, and simple tertiary alkyl radicals through HAT (non-benzylic secondary alkyl radicals were also examined, but moderate yields and enantiomeric ratios were obtained). The HAT catalyst is converted to α-hydroxy radical **C**, which reduces a ligand/Cu^{II}/imine complex (**D**), furnishing Cu-bound benzylic α-amino-α′-oxo radical **E**. Selective combination of this persistent, prochiral radical with the HAT-derived transient alkyl radical occurs preferentially from the less shielded side, yielding amines with high enantiomeric excess. Interestingly, replacing Cu with either Zn, Ni, or Co led to an inverted stereochemical outcome despite the use of the same chiral ligand. This finding was attributed to different coordination geometries around these transition metals. In sharp contrast to the previously published protocol,[28] the reactions of secondary and tertiary benzylic radicals proceeded with excellent stereocontrol (>90% *ee*). The same type of stereoinduction—discrimination between two enantiotopic faces through steric hindrance imposed by a chiral ligand—was also employed to accomplish enantioselective α-hydroxylation of β-keto esters via reaction of a Cu-bound enolate with singlet oxygen.[41]

3. Diastereoselective Transformations

Although there are scores of substrate-controlled Ni- and Cu-catalyzed reactions exhibiting some degree of stereoinduction,[42] this account focuses on those transformations in which various control elements (e.g., stereoelectronic ligand effects) are used to influence and direct the stereochemical outcome of photoredox reactions. In contrast to photoinduced Ni- and Cu-catalyzed enantioselective processes, few experimental and computational mechanistic studies have been devoted to such diastereoselective strategies. This gap in understanding inhibits a full analysis of stereochemical outcomes in these transformations. It is evident that diastereoinduction might result from the intrinsic conformational preferences of the radical species, the steric and electronic nature of both the coupling partner and the ligand system, as well as the rebound capacity of the transition metal catalyst. Notably, the concept of double stereodifferentiation in metallaphotoredox chemistry, wherein the inherent conformational bias of the substrate works in concert with or in opposition to the chiral environment on the transition metal catalyst, appears not to have been explored to any extent.

In addition to detailing stereocontrol at C(sp^3)-hybridized centers, the following discussion also conveys recent developments in the synthesis of stereodefined olefins based on photochemical isomerization.

3.1. Electronic and Structural Features of the Ligand

Recently, we disclosed a ligand-controlled photoredox/Ni dual-catalyzed 1,2-amidoacylation of unactivated olefins for the rapid assembly of nitrogen-containing scaffolds (Scheme 20).

[43] Harnessing proton-coupled electron transfer (PCET),[44] a wide array of amidyl radicals were efficiently coupled with aliphatic and aromatic acyl electrophiles, including in situ activated carboxylic acids, to furnish heterocycles with high degrees of diastereoselectivity. Hammett studies revealed that superior stereoinduction is accomplished with ligand auxiliaries exhibiting higher electron density. This is presumably because of the increased stability of the corresponding acylNi(III) species in the cross-coupling cycle. This unexpected outcome prompted us to conduct density functional theory (DFT) studies investigating this mode of reactivity. Computational evidence supported a mechanistic scenario in which facile oxidative addition of the acyl electrophile with a Ni^0 catalyst precedes a diastereodetermining radical addition to acylNi(II) complex **E**.

In a further study examining the coupling of saccharyl radicals with aryl and heteroaryl bromides,[45] we observed a striking ligand effect on the diastereoselective synthesis of various glycosidic moieties. Replacing the standard ligand, 4,4′-dimethoxy-2,2′-bipyridine (**A**), with phenanthroline (**B**) or 4,4′-di(*tert*-butyl)-2,2′-bipyridine (**C**) improved the dr from 4:1 and 3.3:1 to >20:1, respectively (Scheme 21). Ongoing studies in our group aim to utilize high-throughput screening (HTS) in conjunction with computational tools to unveil the impact of electronic and structural features of diverse ligands on the diastereoselectivity of Ni/photoredox dual catalytic manifolds. This insight is pivotal for future reaction design, thereby granting access to uncharted chemical space.

3.2. Photochemical Isomerization

Harnessing visible-light energy to dictate the stereochemical outcome of synthetic processes is a powerful yet underexplored strategy in organic synthesis. In 2018, Chu disclosed an elegant carbodifunctionalization of alkynes, employing aryl halides and tertiary oxalates to yield trisubstituted (*Z*)-olefins with excellent stereoselectivity (Scheme 22).[46] Mechanistically, the authors propose that photoexcitation of $[Ir\text{-}\{dF(CF_3)ppy\}_2(dtbbpy)]PF_6$ ($E_{1/2}[Ir^{*III}/Ir^{II}]$=+ 1.21 V vs. SCE in MeCN)[47] generates a potent excited triplet state that induces an oxidative fragmentation of the aliphatic oxalate ($E_{1/2}$ =+1.28V vs. SCE for *t*-$BuOCOCO_2Cs$ in MeCN),[46] delivering a tertiary alkyl radical. Upon a regioselective addition to the activated alkyne, the resulting alkenyl radical gets funneled into a Ni-catalyzed cross-coupling cycle to furnish the corresponding (*E*)-alkenyl-Ni^I complex (**E**). This is followed by a key $E \rightarrow Z$ isomerization to deliver the desired product in a photostationary state of equilibrium. As indicated by UV/Vis studies, the initially formed (*E*)-alkene absorbs in the applied wavelength area, promoting double-bond isomerization to its (*Z*)-counterpart. However, the absorption spectrum of the latter does not overlap with the emission bands of the blue light source. As a result, the (*Z*)-olefin is obtained as the exclusive product. To support this hypothesis, the authors demonstrated that (*E*)-alkenes undergo isomerization under visible light in the absence of the Ir catalyst. Control experiments further indicated that light is a vital component of this cross-coupling. In a subsequent study, the same group described the synthesis of *E*- and *Z*-configured 1,4-dienes using a similar photochemical isomerization strategy.[48] Another complementary approach to access stereodefined olefins was reported by Rueping and co-workers.[49] The authors utilized Boc- and Cbz-protected secondary amino acids, as well as a tertiary α-amino acid,

in cross-coupling with diverse aryl electrophiles to yield (*Z*)-alkenes with modest diastereoselectivity.

In addition to alkylarylation, the same group examined a 1,2-carbosulfonylation protocol of alkynes employing sodium sulfinates as radical precursors (Scheme 23).[50] Based on DFT studies, the authors proposed a mechanistic scenario starting with radical addition to a low-valent Ni^0 complex followed by 1,2-migratory insertion of the alkyne. At this point, a Ni-controlled *anti/syn* isomerization takes place. Subsequent oxidative addition of the aryl electrophile and reductive elimination from Ni^{III} species **I** give rise to *anti*-addition olefin products. Although both *anti*- and *syn*-addition products display energetically similar profiles, the implementation of diverse photocatalysts exhibiting distinct triplet state energies proved fruitful in tuning stereochemical outcomes. For example, an Ir^{III} catalyst with a higher triplet state energy than the initially formed *anti*-addition product can induce double-bond isomerization via energy transfer (ET), yielding the opposite isomer. However, a superior energy profile of the latter compared with the photocatalyst is required. These results highlight that a key prerequisite for the continued success of this catalytic paradigm is the discovery of photocatalysts harboring a diverse range of triplet state energies.

4. Conclusion and Outlook

In recent years, metallaphotoredox catalysis has emerged as an enabling technology to install C(sp^3)-hybridized centers under mild reaction conditions. High-energy radical intermediates, obtained through SET-induced oxidative or reductive fragmentation modes, are funneled into a metal catalytic cycle for further functionalization. Although substantial effort has been devoted to the study of photoinduced, stereocontrolled Ni- or Cu-catalyzed transformations, numerous synthetic challenges remain, and considerable mechanistic ambiguity persists in this research arena as well. Particular opportunities for advancement include:

1. Incorporation of sophisticated computational, spectroscopic, and mechanistic studies to explore the energetics of transient open-shell species and the engagement of radicals with organometallic complexes.
2. To date, the pool of radical precursors amenable to stereoselective transformations is largely limited to stabilized radicals (e.g., α-amino, α-alkoxy, or benzylic systems). The incorporation of non-stabilized as well as heteroatom-based counterparts in pathways involving radical addition to the transition-metal center is highly desirable, particularly those of enantioselective C(sp^3)–C(sp^3) cross-couplings.
3. Success in enantioselective photoredox-promoted cross-coupling is challenging because the ligands are largely responsible for both yields and enantioinduction. Ligand characteristics contributing to these two outcomes are often at odds with one another, and yet they must be concertedly optimized. Discovering a single ligand or even class of ligands that would be ideal for all coupling partners would appear challenging, if not impossible. For the foreseeable future, empirical

explorations combined with high-throughput experimentation may provide the best way forward to rewarding results.

4. Currently, stereoselective multicomponent reactions are largely restricted to activated alkenes and alkynes. The development of strategies to incorporate unactivated and highly substituted C–C π-bonds would further expand this field.

5. Perhaps the most underappreciated/underdeveloped aspect of photoredox-mediated cross-coupling reactions is the ability to control diastereoselectivity through the proper choice of ligands on the transition metal. Thus, the reversible engagement of radicals with the transition metal complexes provides opportunities for dynamic kinetic resolutions to induce high levels of diastereoselectivity—a very rare attribute among current cross-coupling methods.

6. Finally, the exploitation of emerging base metals, including chromium,[51] in photoinduced stereoselective transformations presents new avenues for novel reactivity modes. Clearly, exciting possibilities await further exploration of stereocontrol in photoredox cross-coupling reactions.

Acknowledgements

The authors acknowledge financial support provided by NIGMS (R35 GM 131680 to G.M.). Dr. Alexander Lipp is grateful to the Deutsche Forschungsgemeinschaft (DFG) for a postdoctoral fellowship (LI 3682/1-1). The authors thank their colleague Borna Saeednia (University of Pennsylvania) for providing the photographical art used in the frontispiece.

Biography

Alexander Lipp studied biomedical chemistry at Johannes Gutenberg University in Mainz. After a research stay in the group of Professor Steven P. Armes at the University of Sheffield, he returned to Mainz, where he earned his PhD in organic chemistry working in the laboratory of Professor Till Opatz. He is currently a postdoctoral researcher (DFG fellow) in the group of Professor Gary A. Molander at the University of Pennsylvania.

Shorouk Badir earned her A.B. in chemistry from Bryn Mawr College in 2016 under the supervision of Professor William P. Malachowski. She then joined the laboratory of Professor Gary A. Molander at the University of Pennsylvania, where she is currently

pursuing her PhD. She is actively engaged in developing new transformations using photoredox catalysis.

Gary Molander completed his undergraduate studies in chemistry at Iowa State University under the tutelage of Professor Richard C. Larock. He earned his PhD at Purdue University with Professor Herbert C. Brown and undertook postdoctoral training with Professor Barry M. Trost at the University of Wisconsin, Madison. He began his academic career at the University of Colorado, Boulder, moving to the University of Pennsylvania in 1999, where he is currently the Hirschmann-Makineni Professor of Chemistry.

References

[1]. a)Tellis JC, Primer DN, Molander GA, Science 2014, 345, 433–436; [PubMed: 24903560] b)Zuo Z, Ahneman DT, Chu L, Terrett JA, Doyle AG, MacMillan DW, Science 2014, 345, 437–440; [PubMed: 24903563] c)Primer DN, Karakaya I, Tellis JC, Molander GA, J. Am. Chem. Soc 2015, 137, 2195–2198; [PubMed: 25650892] d)Shields BJ, Doyle AG, J. Am. Chem. Soc 2016, 138, 12719–12722. [PubMed: 27653738] e)For selected reviews, please see: Tellis JC, Kelly CB, Primer DN, Jouffroy M, Patel NR, Molander GA, Acc. Chem. Res 2016, 49, 1429–1439; [PubMed: 27379472] f)Skubi KL, Blum TR, Yoon TP, Chem. Rev 2016, 116, 10035–10074; [PubMed: 27109441] g)Milligan JA, Phelan JP, Badir SO, Molander GA, Angew. Chem. Int. Ed 2019, 58, 6152–6163; *Angew. Chem.* 2019, 131, 6212–6224;h)Twilton J, Le C, Zhang P, Shaw MH, Evans RW, MacMillan DWC, Nat. Rev. Chem 2017, 1, 0052;i)Matsui JK, Lang SB, Heitz DR, Molander GA, ACS Catal 2017, 7, 2563–2575; [PubMed: 28413692] j)Parasram M, Gevorgyan V, Chem. Soc. Rev 2017, 46, 6227–6240. [PubMed: 28799591]

[2]. a)Lovering F, Bikker J, Humblet C, J. Med. Chem 2009, 52, 6752–6756; [PubMed: 19827778] b)Lovering F, MedChemComm 2013, 4, 515–519.

[3]. a)For selected examples of complementary radical-based asymmetric Ni- and Cu-catalyzed transformations, please see: Zhao Y, Weix DJ, J. Am. Chem. Soc 2015, 137, 3237–3240; [PubMed: 25716775] b)Gu Q-S, Li Z-L, Liu X-Y, Acc. Chem. Res 2020, 53, 170–181; [PubMed: 31657546] c)Li Z-L, Fang G-C, Gu Q-S, Liu X-Y, Chem. Soc. Rev 2020, 49, 32–48; [PubMed: 31802082] d)Poremba KE, Dibrell SE, Reisman SE, ACS Catal 2020, 10, 8237–8246. [PubMed: 32905517] e)For recent reviews on enantioselective reactions in photoinduced systems, please see: Busch J, Knoll DM, Zippel C, Bräse S, Bizzarri C, Dalton Trans 2019, 48, 15338–15357; [PubMed: 31573576] f)Zhang H-H, Chen H, Zhu C, Yu S, Sci. China Chem 2020, 63, 637–647.

[4]. Hartwig JF, Organotransition Metal Chemistry: from Bonding to Catalysis, University Science Books, Sausalito, Calif., 2010.

[5]. Gutierrez O, Tellis JC, Primer DN, Molander GA, Kozlowski MC, J. Am. Chem. Soc 2015, 137, 4896–4899. [PubMed: 25836634]

[6]. Ryu D, Primer DN, Tellis JC, Molander GA, Chem. Eur. J 2016, 22, 120–123. [PubMed: 26550805]

[7]. Amani J, Sodagar E, Molander GA, Org. Lett 2016, 18, 732–735. [PubMed: 26828576]

[8]. Stache EE, Rovis T, Doyle AG, Angew. Chem. Int. Ed 2017, 56, 3679–3683; *Angew. Chem.* 2017, 129, 3733–3737.

[9]. Zhou Q-Q, Lu F-D, Liu D, Lu L-Q, Xiao W-J, Org. Chem. Front 2018, 5, 3098–3102.

[10]. Zuo Z, Cong H, Li W, Choi J, Fu GC, MacMillan DW, J. Am. Chem. Soc 2016, 138, 1832–1835. [PubMed: 26849354]

[11]. Pezzetta C, Bonifazi D, Davidson RWM, Org. Lett 2019, 21, 8957–8961. [PubMed: 31647246]
[12]. Godula K, Sames D, Science 2006, 312, 67–72. [PubMed: 16601184]
[13]. Ahneman DT, Doyle AG, Chem. Sci 2016, 7, 7002–7006. [PubMed: 28058105]
[14]. Shen Y, Gu Y, Martin R, J. Am. Chem. Soc 2018, 140, 12200–12209. [PubMed: 30184423]
[15]. Rand AW, Yin H, Xu L, Giacoboni J, Martin-Montero R, Romano C, Montgomery J, Martin R, ACS Catal 2020, 10, 4671–4676.
[16]. Cheng X, Lu H, Lu Z, Nat. Commun 2019, 10, 3549. [PubMed: 31391466]
[17]. Heitz DR, Tellis JC, Molander GA, J. Am. Chem. Soc 2016, 138, 12715–12718. [PubMed: 27653500]
[18]. Guan H, Zhang Q, Walsh PJ, Mao J, Angew. Chem. Int. Ed 2020, 59, 5172–5177; *Angew. Chem.* 2020, 132, 5210–5215.
[19]. Ding W, Lu LQ, Zhou QQ, Wei Y, Chen JR, Xiao WJ, J. Am. Chem. Soc 2017, 139, 63–66. [PubMed: 28001382]
[20]. Gandolfo E, Tang X, Raha Roy S, Melchiorre P, Angew. Chem. Int. Ed 2019, 58, 16854–16858; *Angew. Chem.* 2019, 131, 17010–17014.
[21]. Fan P, Lan Y, Zhang C, Wang C, J. Am. Chem. Soc 2020, 142, 2180–2186. [PubMed: 31971787]
[22]. a)Hossain A, Bhattacharyya A, Reiser O, Science 2019, 364, eaav9713; [PubMed: 31048464] b)Zhong M, Pannecoucke X, Jubault P, Poisson T, Beilstein J. Org. Chem 2020, 16, 451–481;c)Kancherla R, Muralirajan K, Sagadevan A, Rueping M, Trends Chem 2019, 1, 510–523;d)Nicholls TP, Bissember AC, Tetrahedron Lett 2019, 60, 150883;e)Reiser O, Acc. Chem. Res 2016, 49, 1990–1996. [PubMed: 27556932]
[23]. Kainz QM, Matier CD, Bartoszewicz A, Zultanski SL, Peters JC, Fu GC, Science 2016, 351, 681–684. [PubMed: 26912852]
[24]. Fu GC, ACS Cent. Sci 2017, 3, 692–700. [PubMed: 28776010]
[25]. Guo Q, Wang M, Peng Q, Huo Y, Liu Q, Wang R, Xu Z, ACS Catal 2019, 9, 4470–4476.
[26]. Wang F, Wang D, Wan X, Wu L, Chen P, Liu G, J. Am. Chem. Soc 2016, 138, 15547–15550. [PubMed: 27934001]
[27]. Zhang Y, Sun Y, Chen B, Xu M, Li C, Zhang D, Zhang G, Org. Lett 2020, 22, 1490–1494. [PubMed: 32027141]
[28]. Li Y, Zhou K, Wen Z, Cao S, Shen X, Lei M, Gong L, J. Am. Chem. Soc 2018, 140, 15850–15858. [PubMed: 30372057]
[29]. Han B, Li Y, Yu Y, Gong L, Nat. Commun 2019, 10, 3804. [PubMed: 31444326]
[30]. McLean EB, Lee A-L, Tetrahedron 2018, 74, 4881–4902.
[31]. Perepichka I, Kundu S, Hearne Z, Li C-J, Org. Biomol. Chem 2015, 13, 447–451. [PubMed: 25372475]
[32]. Querard P, Perepichka I, Zysman-Colman E, Li C-J, Beilstein J. Org. Chem 2016, 12, 2636–2643. [PubMed: 28144334]
[33]. Lu F-D, Liu D, Zhu L, Lu L-Q, Yang Q, Zhou Q-Q, Wei Y, Lan Y, Xiao W-J, J. Am. Chem. Soc 2019, 141, 6167–6172. [PubMed: 30929425]
[34]. Wang D, Zhu N, Chen P, Lin Z, Liu G, J. Am. Chem. Soc 2017, 139, 15632–15635. [PubMed: 29039930]
[35]. Sha W, Deng L, Ni S, Mei H, Han J, Pan Y, ACS Catal 2018, 8, 7489–7494.
[36]. Wang T, Wang Y-N, Wang R, Zhang B-C, Yang C, Li Y-L, Wang X-S, Nat. Commun 2019, 10, 5373. [PubMed: 31772198]
[37]. Chen J, Wang P-Z, Lu B, Liang D, Yu X-Y, Xiao W-J, Chen J-R, Org. Lett 2019, 21, 9763–9768. [PubMed: 31746212]
[38]. Bao X, Wang Q, Zhu J, Angew. Chem. Int. Ed 2019, 58, 2139–2143; *Angew. Chem.* 2019, 131, 2161–2165.
[39]. Cheng Z, Chen PH, Liu GS, Acta Chim. Sin. (Engl. Ed.) 2019, 77, 856–860.
[40]. Li Y, Lei M, Gong L, Nat. Catal 2019, 2, 1016–1026.
[41]. Yang F, Zhao J, Tang X, Wu Y, Yu Z, Meng Q, Adv. Synth. Catal 2019, 361, 1673–1677.

[42]. a)For selected examples of substrate-controlled photoinduced Ni-catalyzed diastereoselective transformations, please see: Srnith RT, Zhang XH, Rincon JA, Agejas J, Mateos C, Barberis M, Garcia-Cerrada S, de Frutos O, MacMillan DWC, J. Am. Chem. Soc 2018, 140, 17433–17438; [PubMed: 30516995] b)Kautzky JA, Wang T, Evans RW, MacMillan DWC, J. Am. Chem. Soc 2018, 140, 6522–6526; [PubMed: 29754491] c)Badir SO, Dumoulin A, Matsui JK, Molander GA, Angew. Chem. Int. Ed 2018, 57, 6610–6613; *Angew. Chem.* 2018, 130, 6720–6723.d)For selected examples on diastereoselective Cu- or photoredox/Cu-catalyzed transformations, please see: Hossain A, Engl S, Lutsker E, Reiser O, ACS Catal 2019, 9, 1103–1109;e)Rawner T, Lutsker E, Kaiser CA, Reiser O, ACS Catal 2018, 8, 3950–3956;f)Wang C, Yu Y, Liu W-L, Duan W-L, Org. Lett 2019, 21, 9147–9152; [PubMed: 31670519] g)Smirnov VO, Maslov AS, Kokorekin VA, Korlyukov AA, Dilman AD, Chem. Commun 2018, 54, 2236–2239;h)Gao X-W, Meng Q-Y, Xiang M, Chen B, Feng K, Tung C-H, Wu L-Z, Adv. Synth. Catal 2013, 355, 2158–2164. For a more general overview of photoinduced Cu-catalyzed transformations, please refer to the review articles cited herein: [22a] and [22e].

[43]. Zheng S, Zhang S-Q, Saeednia B, Zhou J, Anna JM, Hong X, Molander GA, Chem. Sci 2020, 11, 4131–4137.

[44]. Choi GJ, Knowles RR, J. Am. Chem. Soc 2015, 137, 9226–9229. [PubMed: 26166022]

[45]. Dumoulin A, Matsui JK, Gutierrez-Bonet A, Molander GA, Angew. Chem. Int. Ed 2018, 57, 6614–6618; *Angew. Chem.* 2018, 130, 6724–6728.

[46]. Guo L, Song F, Zhu S, Li H, Chu L, Nat. Commun 2018, 9, 4543. [PubMed: 30382103]

[47]. Kelly CB, Patel NR, Primer DN, Jouffroy M, Tellis JC, Molander GA, Nat. Protoc 2017, 12, 472–492. [PubMed: 28151464]

[48]. Song F, Wang F, Guo L, Feng X, Zhang Y, Chu L, Angew. Chem. Int. Ed 2020, 59, 177–181; *Angew. Chem.* 2020, 132, 183–187.

[49]. Yue H, Zhu C, Kancherla R, Liu F, Rueping M, Angew. Chem. Int. Ed 2020, 59, 5738–5746; *Angew. Chem.* 2020, 132, 5787–5795.

[50]. Zhu C, Yue H, Maity B, Atodiresei I, Cavallo L, Rueping M, Nat. Catal 2019, 2, 678–687.

[51]. a)For selected examples of Cr-catalyzed stereoselective transformations, see: Schwarz JL, Schäfers F, Tlahuext-Aca A, Lückemeier L, Glorius F, J. Am. Chem. Soc 2018, 140, 12705–12709; [PubMed: 30216059] b)Schwarz JL, Kleinmans R, Paulisch TO, Glorius F, J. Am. Chem. Soc 2020, 142, 2168–2174; [PubMed: 31923360] c)Mitsunuma H, Tanabe S, Fuse H, Ohkubo K, Kanai M, Chem. Sci 2019, 10, 3459–3465. [PubMed: 30996935]

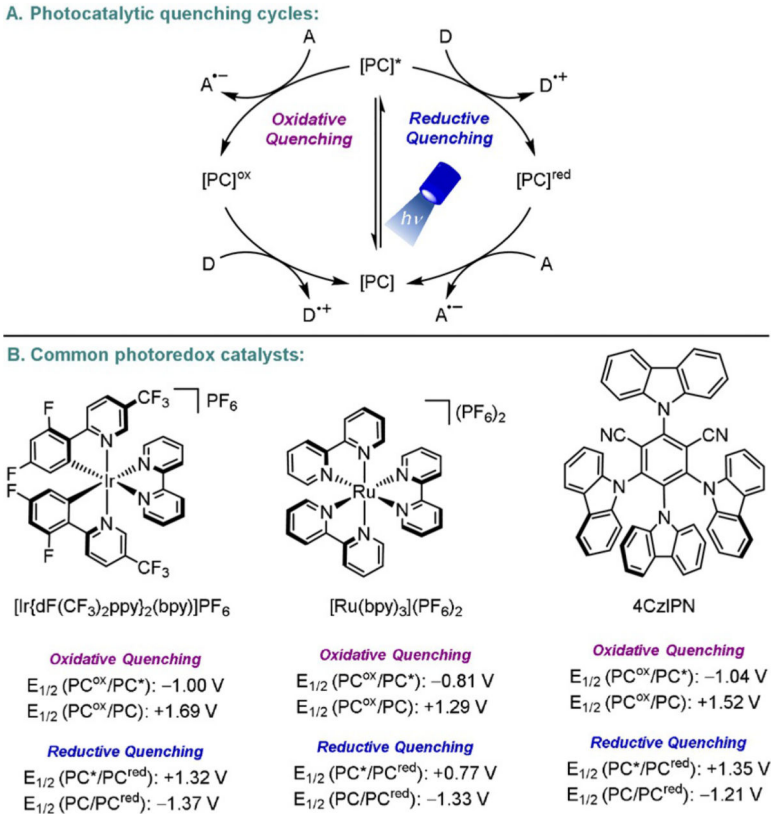

Figure 1.

A) Photocatalytic quenching cycles and B) three common photoredox catalysts.

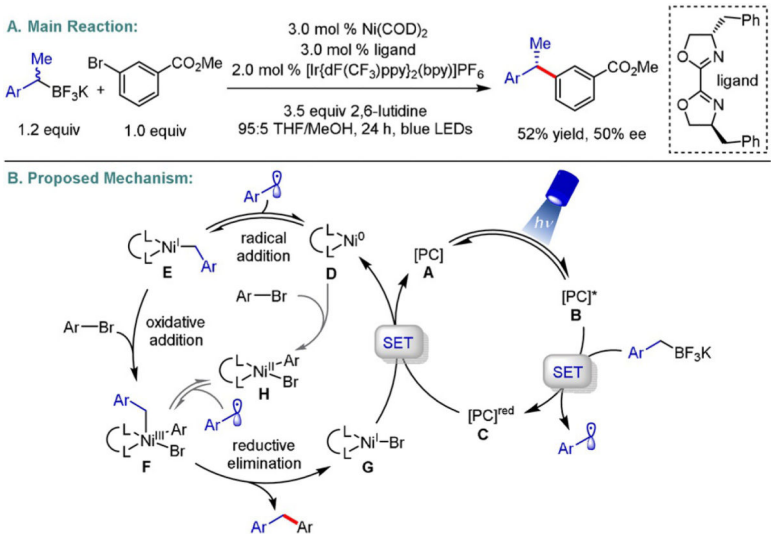

Scheme 1.

Enantioselective photoredox/Ni dual-catalyzed cross-coupling of benzyltrifluoroborates.

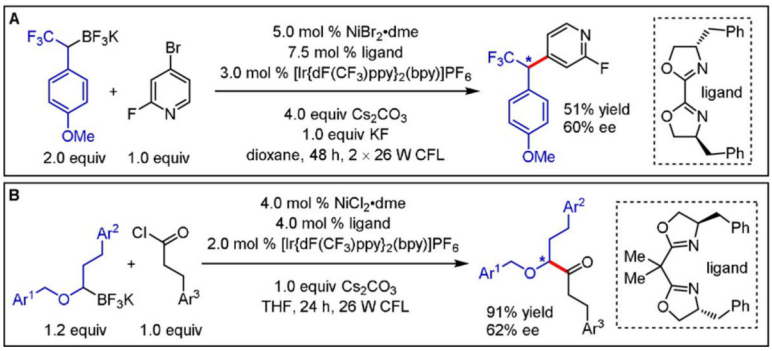

Scheme 2.

Enantioselective photoredox/Ni dual-catalyzed cross-coupling of A) α-trifluoromethyltrifluoroborates and B) α-alkoxymethyltrifluoroborates.

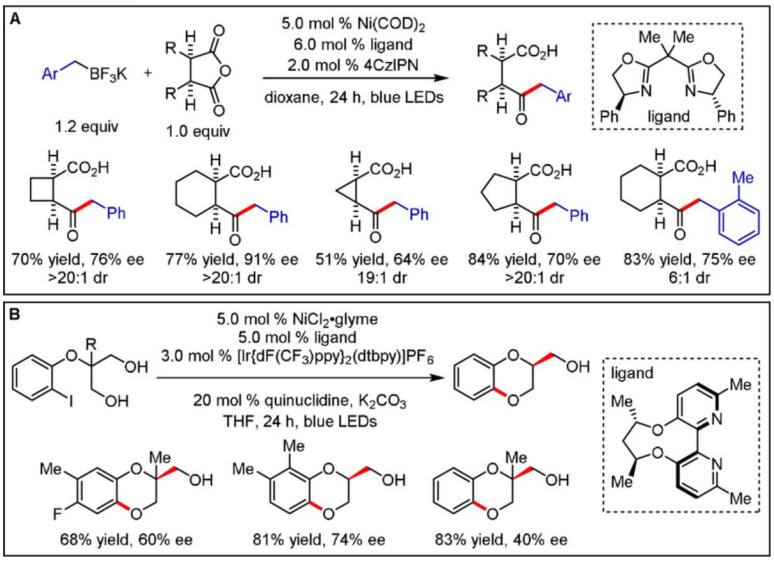

Scheme 3.

Enantioselective photoredox/Ni dual-catalyzed desymmetrization of A) cyclic *meso* anhydrides and B) diols.

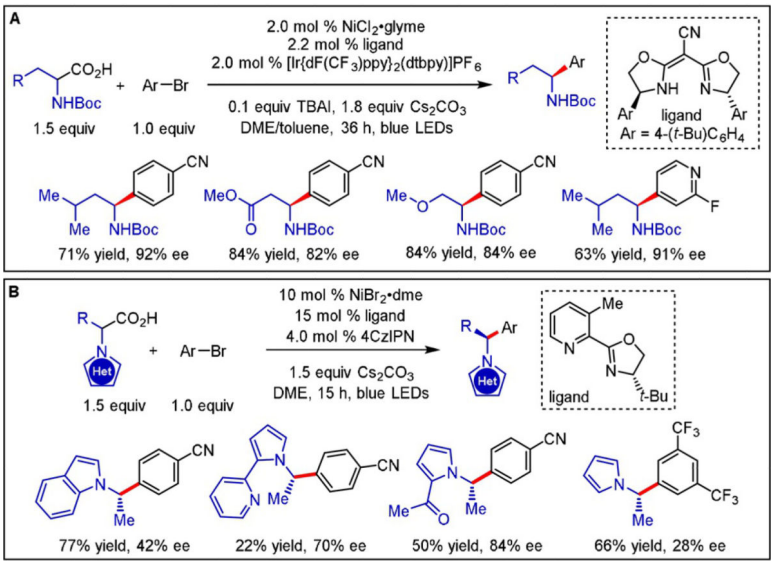

Scheme 4.

Enantioselective photoredox/Ni dual-catalyzed decarboxylative arylations.

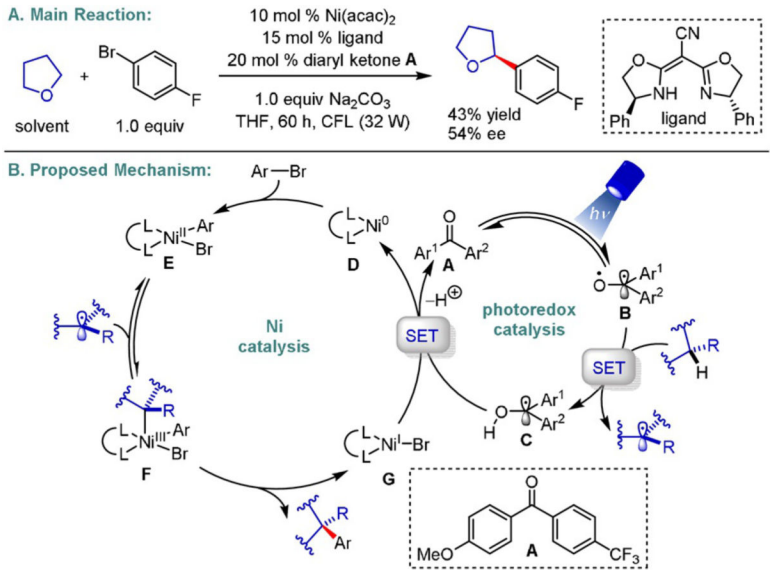

Scheme 5.

Enantioselective photoredox/Ni dual-catalyzed C(sp^3)-H arylation.

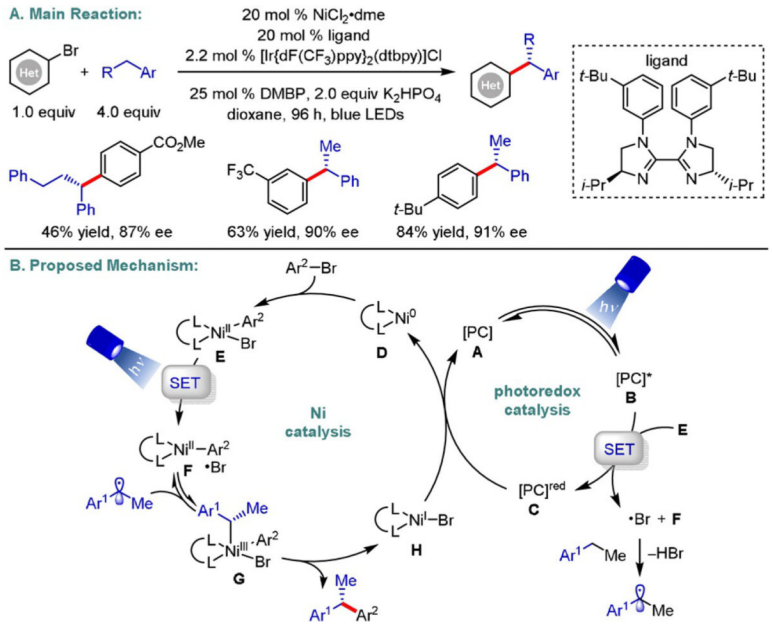

Scheme 6.

Enantioselective photoredox/Ni dual-catalyzed C(sp^3)-H arylation.

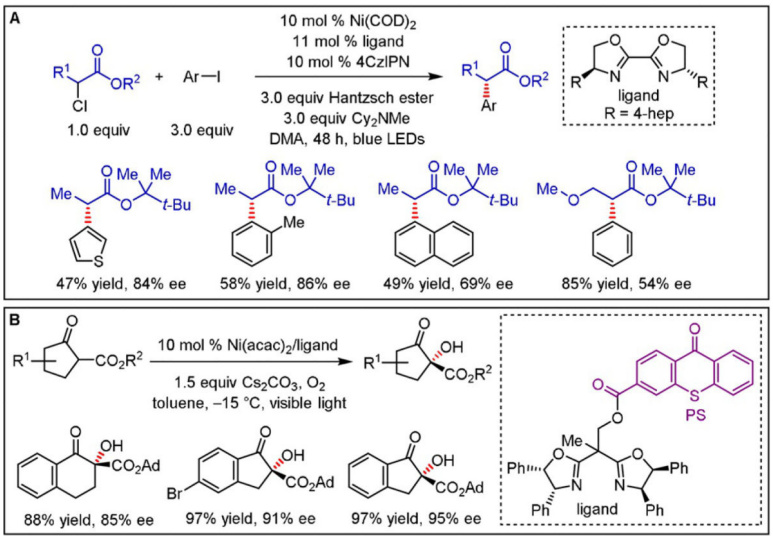

Scheme 7.

A) Enantioselective photoredox/Ni dual-catalyzed arylation of α-chloro esters and B) photoinduced enantioselective oxidation of β-ketoesters and β-ketoamides.

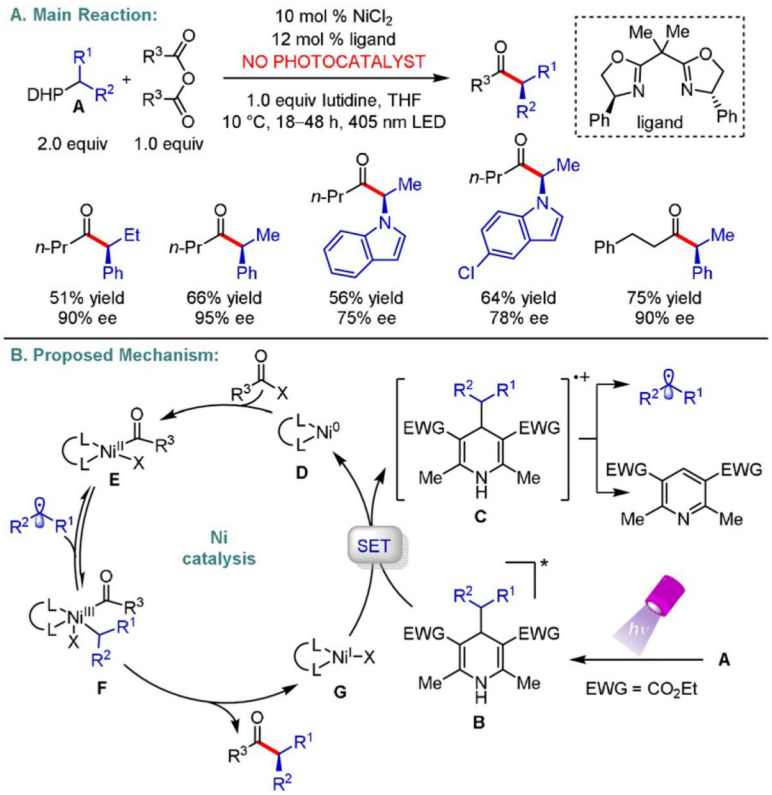

Scheme 8.

Enantioselective photochemical Ni-catalyzed acylation using 1,4-DHPs.

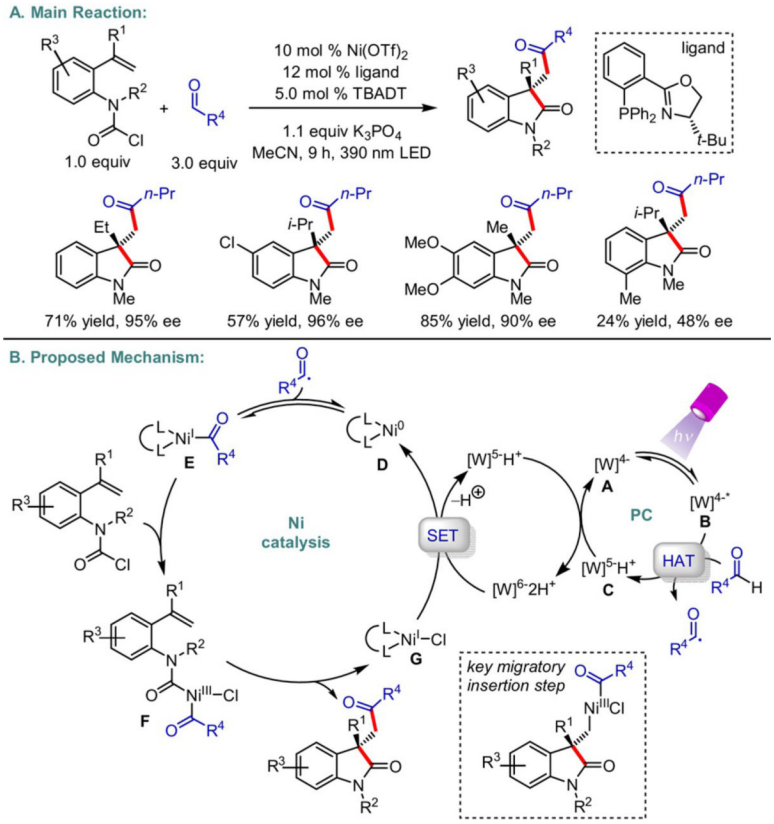

Scheme 9.

Enantioselective photoredox/Ni dual-catalyzed 1,2-carbodifunctionalization of carbamoyl chloride-tethered alkenes.

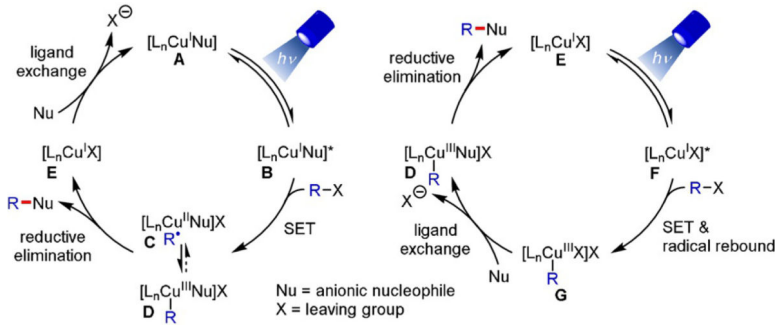

Scheme 10.

Mechanism involving photoexcitation of a Cu^{I} complex and reductive elimination from Cu^{III}.

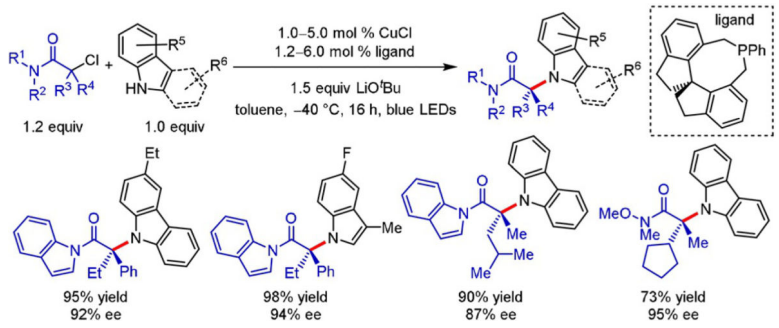

Scheme 11.

Enantioselective C-N cross-coupling of tertiary α-chloroamides with carbazoles and indoles.

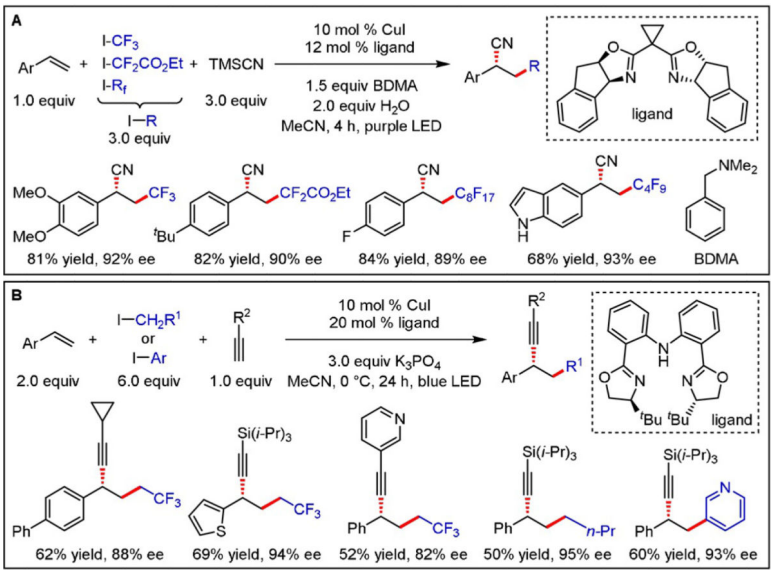

Scheme 12.

Interposing a Giese-type addition prior to formation of the Cu^{III} intermediate enables A) cyanation/fluoroalkylation and B) alkylation/alkynylation or arylation/alkynylation of alkenes.

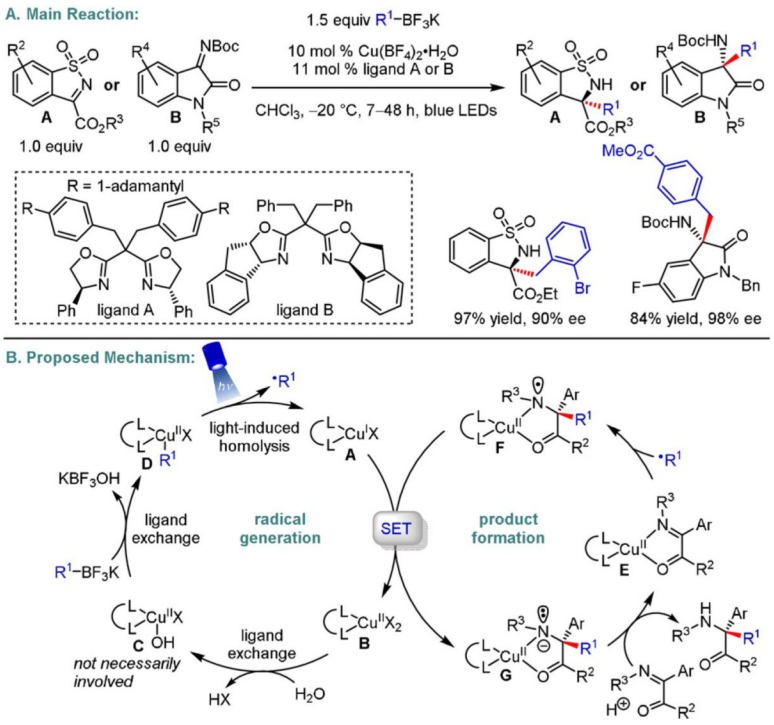

Scheme 13.

Enantioselective alkylation of *N*-sulfonylimines and selected ketimines.

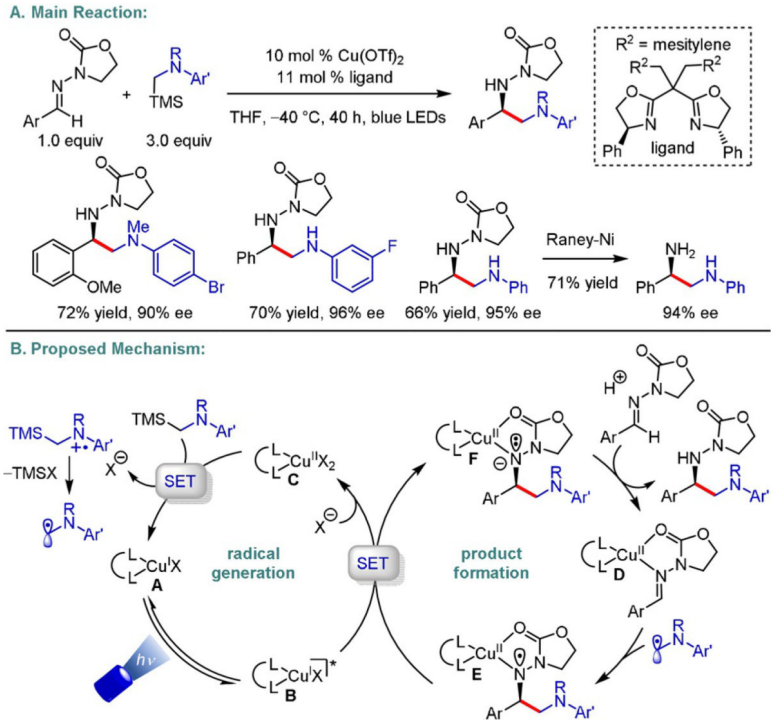

Scheme 14.

Enantioselective α-aminoalkylation of *N*-acylhydrazones.

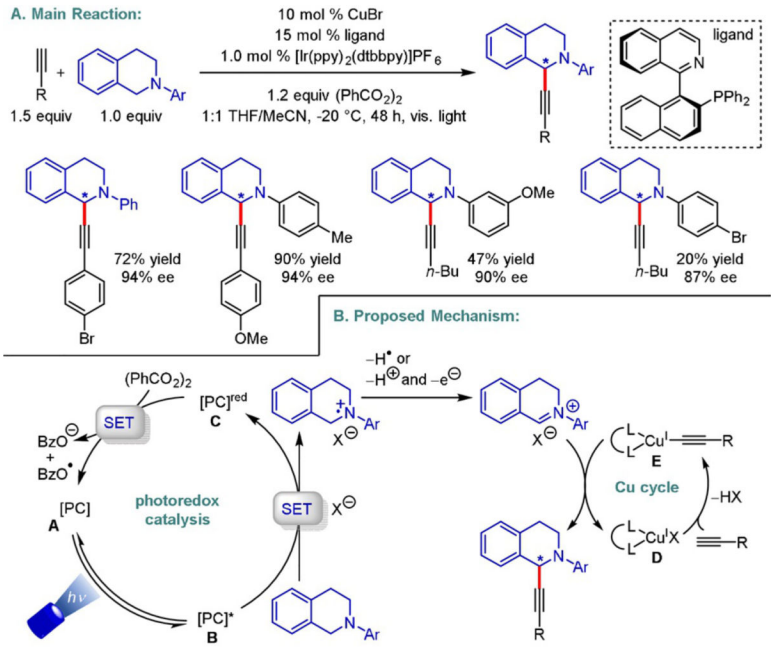

Scheme 15.

Enantioselective alkynylation of *N*-aryl-1,2,3,4-tetrahydroisoquinolines.

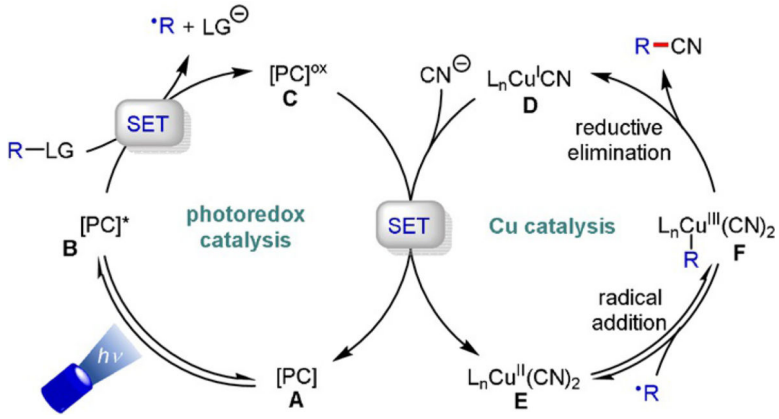

Scheme 16.

Proposed mechanism for Cu/photoredox dual-catalyzed enantioselective cyanations.

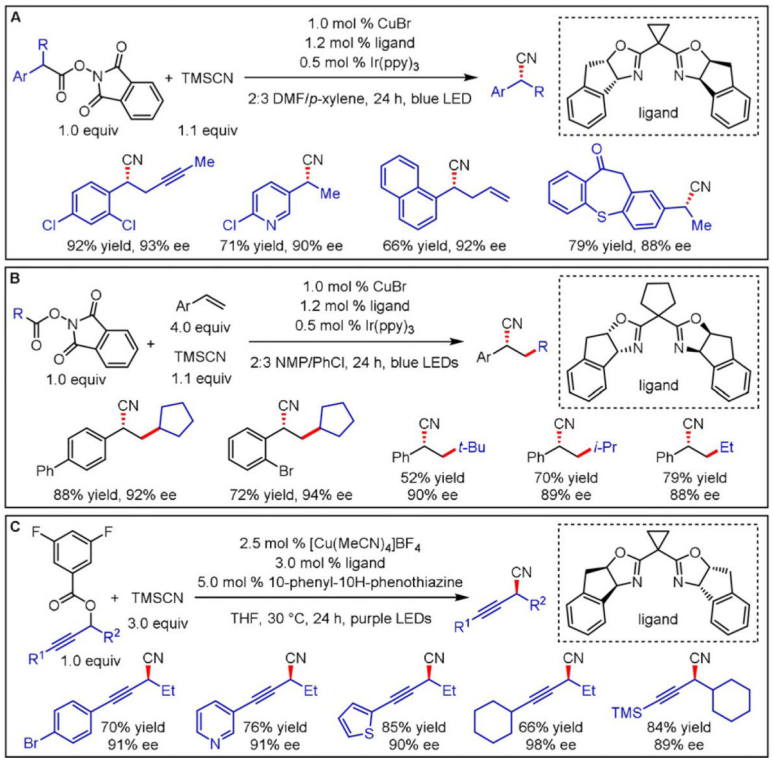

Scheme 17.

Enantioselective cyanations using redox-active esters as radical precursors.

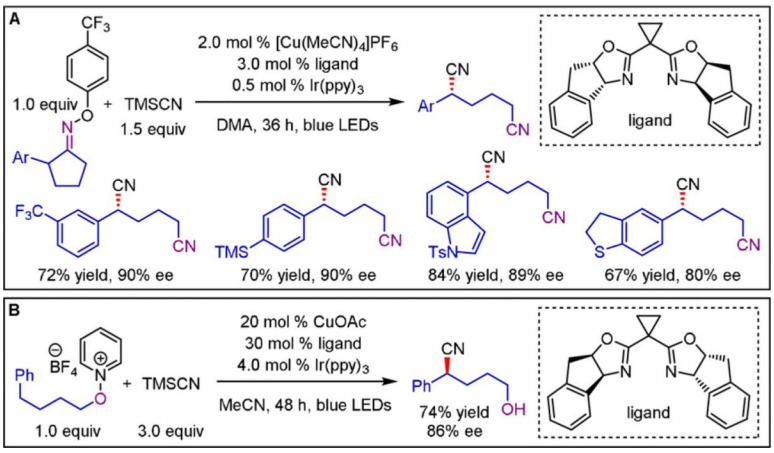

Scheme 18.

Enantioselective cyanations using A) oxime esters and B) *N*-alkoxypyridinium salts as radical precursors.

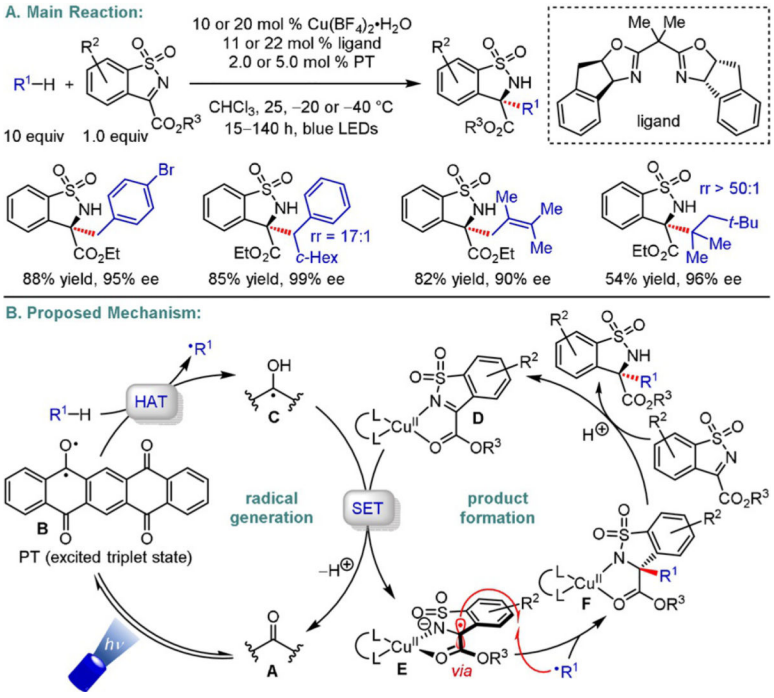

Scheme 19.

Enantioselective alkylation of *N*-sulfonylimines.

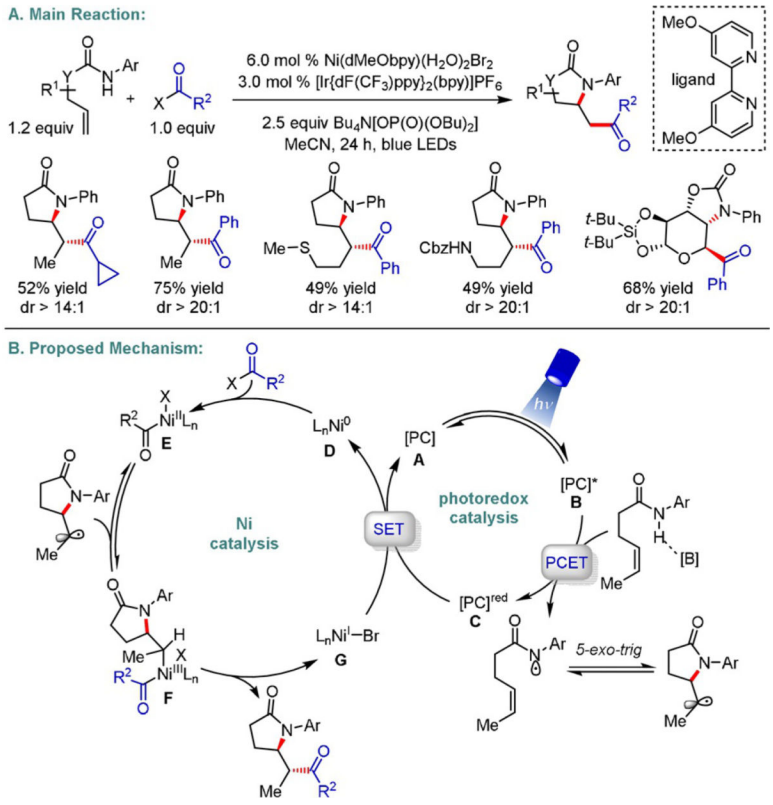

Scheme 20.

Diastereoselective photoredox/Ni dual-catalyzed 1,2-amidoacylation.

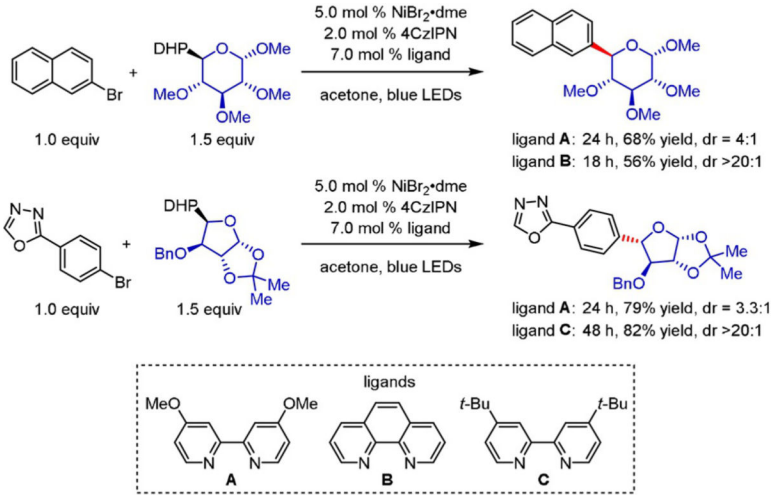

Scheme 21.

Diastereoselective photoredox/Ni dual-catalyzed arylation of saccharide-based DHPs.

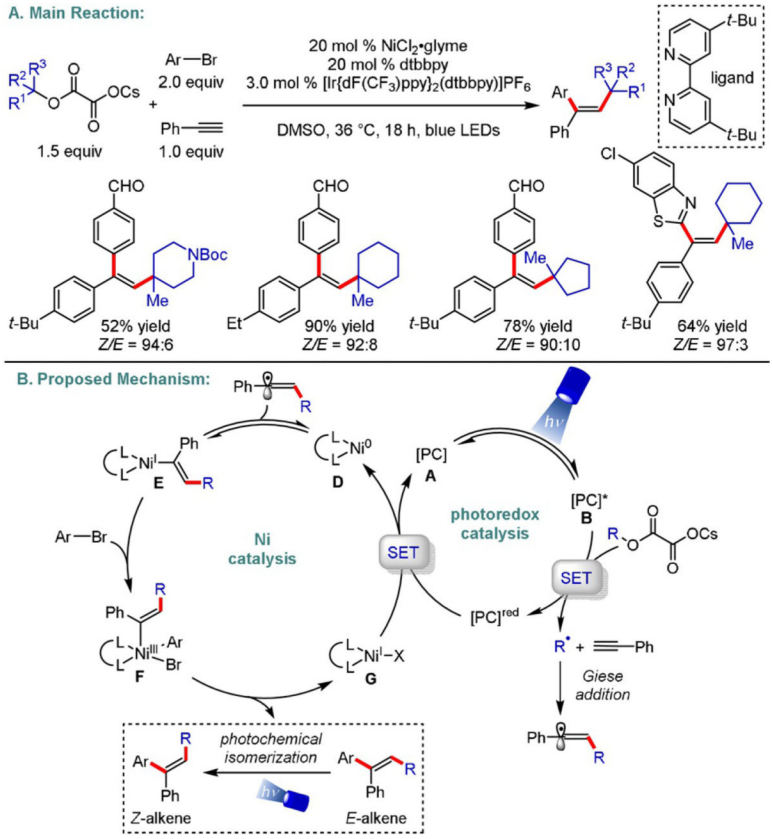

Scheme 22.

Diastereoselective photoredox/Ni dual-catalyzed alkylarylation of alkynes.

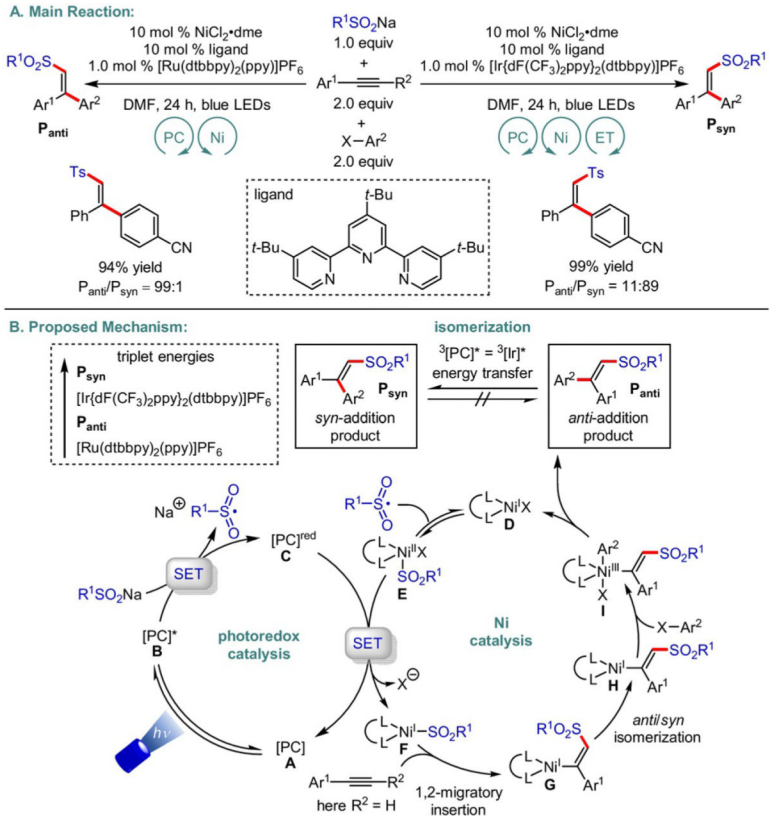

Scheme 23.

Diastereoselective photoredox/Ni dual-catalyzed 1,2-carbosulfonylation of alkynes.